Cellular and Molecular Life Sciences (2025) 82:148
https://doi.org/10.1007/s00018-025-05679-9

ORIGINAL ARTICLE

S146 and M148 within the mature chain domain of PSMB4 are crucial for degrading PRRSV nsp1α

Binghua Chen[1,2] · Yongjie Chen[1] · Zhan He[1] · Yanfei Pan[1] · Yunyan Luo[1] · Jiecong Yan[1] · Fangfang Li[1] · Chunhe Guo[1]

Received: 27 November 2024 / Revised: 23 December 2024 / Accepted: 25 March 2025

Abstract

Porcine reproductive and respiratory syndrome virus (PRRSV) is a single-stranded positive-sense RNA virus with an envelope. It-encoded non-structural protein 1α (nsp1α) plays a key role in evading host immune responses. Exploring the interaction between host factors and PRRSV nsp1α is crucial for understanding the mechanism of virus immune escape and virus control. Here, we constructed a cDNA library using porcine lung tissues and identified 33 potential host proteins interacting with viral nsp1α using yeast two-hybrid (Y2H) screening. These interactions were further analyzed using Gene Ontology and KEGG pathway analysis. Confocal microscopy revealed that proteasome subunit beta type-4 (PSMB4), carnosine dipeptidase 2 (CNDP2) and poly(rC) binding protein 1 (PCBP1) colocalized with viral nsp1α. The interaction between PSMB4 and nsp1α was further confirmed by Y2H and co-immunoprecipitation. PRRSV infection did not affect PSMB4 expression in both Marc-145 cells and porcine alveolar macrophages (PAMs). Overexpression of PSMB4 reduced nsp1α protein levels in a dose-dependent manner and decreased the accumulation of both viral N and nsp1α proteins in the context of PRRSV infection, while its knockdown promoted PRRSV replication. These data suggest that PSMB4 is a host restriction factor for PRRSV. Structure prediction and truncated mutant assays found that S146 and M148 within the mature chain domain of PSMB4 were crucial for binding and degrading nsp1α. These findings suggest that PRRSV nsp1α interacts with host proteins, with PSMB4 specifically binding to degrade nsp1α, thereby inhibiting PRRSV replication.

Keywords Yeast two-hybrid screening · PRRSV · Nsp1α · PSMB4 · Virus-host interactions

Introduction

Porcine reproductive and respiratory syndrome virus (PRRSV) is a major pathogen causing significant economic losses in swine populations worldwide. It primarily affects pigs' respiratory and reproductive systems, causing disease in piglets and reproductive failure in breeding animals. PRRSV has two main species: PRRSV-1 (European type) and PRRSV-2 (North American type), with multiple strains of varying virulence and geographical distribution [1–3]. Both species encode nonstructural proteins (nsps) essential for viral replication and immune evasion. The virus's high mutation rate complicates vaccine development and disease control [4]. Mutation driven by gene recombination continues to threaten the global swine industry, leading to substantial economic losses.

PRRSV is a single-stranded, positive-sense RNA virus. Its genome is approximately 15 kb in length, belonging to the Arteriviridae family. The genome contains 10–12 open reading frames (ORFs) that encode at least 16 nonstructural proteins and 8 structural proteins: GP2, GP3, GP4, GP5, ORF5a, envelope (E), matrix (M), and nucleocapsid (N) proteins [5]. The nonstructural proteins are encoded by two large ORFs: ORF1a and ORF1b, which produce the replicase polyproteins pp1a and pp1b. These polyproteins are cleaved into 14 nsps by viral proteases, nsp1α, nsp1β,

Binghua Chen, Yongjie Chen and Zhan He contributed equally to this work.

✉ Chunhe Guo
guochunh@mail.sysu.edu.cn

[1] Guangdong Laboratory for Lingnan Modern Agriculture, State Key Laboratory for Animal Disease Control and Prevention, Key Laboratory of Zoonosis Prevention and Control of Guangdong Province, College of Veterinary Medicine, South China Agricultural University, Guangzhou, Guangdong, PR China

[2] College of Henry Fork School of Biology and Agriculture, Shaoguan University, Daxue Road, Zhenjiang District, Shaoguan 512005, China

Published online: 07 April 2025

nsp2 and nsp4. Specifically, nsp1α, nsp1β, nsp2, nsp3, nsp4, nsp5, nsp6, nsp7α, nsp7β and nsp8 are generated from pp1a, while pp1b is cleaved into nsp9, nsp10, nsp11 and nsp12 [6–8].

PRRSV nsps are the first proteins synthesized during infection, crucial for regulating viral RNA synthesis, replication and immune responses. Nsp1α, nsp1β, nsp2, nsp4 and nsp11 inhibit type I interferon responses [9–11]. Nsp1 has two papain-like cysteine protease (PCP) domains that self-cleave to produce nsp1α and nsp1β [12, 13]. Nsp1α is released by cleavage at Met180/Ala181 and performs functions such as sub-genomic RNA synthesis, viral transcription, virion biogenesis, polyprotein processing and regulation of type I interferon gene expression [14–16]. Nsp1α interacts with immune signaling proteins IRF3 and IRF7, preventing their activation and nuclear translocation [17]. It also inhibits tripartite motif containing 25 (TRIM25) activity, blocking RIG-I activation and downstream interferon responses [18]. Nsp1α modulates NF-κB signaling by interacting with IKK and other adaptors, impairing inflammatory responses. By interfering with NEMO, nsp1α suppresses NF-κB signaling and immune responses, enhancing viral replication [10]. RELB in the non-canonical NF-κB pathway may be targeted by PRRSV to disrupt immune defenses and promote viral persistence [19]. Additionally, nsp1α interacts with apoptosis-related proteins, promoting cell survival or inhibiting antiviral-induced cell death [20].

The proteasome is a major complex responsible for degrading most misfolded proteins and pathogens within the organism [21, 22]. Proteasome subunit beta type-4 (PSMB4) is a non-catalytic component of the proteasome 20 S core subunit complex. PSMB4 is localized to both the cell nucleus and cytoplasm, where it plays a key role in regulating proteasome activity for the proteolytic degradation of intracellular proteins. As a member of the evolutionarily conserved PSMB protein family, PSMB4 is a multifunctional protein involved in processes such as protein degradation, immune regulation and antigen processing [23–25].

The molecular mechanism of PRRSV nsp1α interaction with host proteins and its role in regulating PRRSV replication remains unclear. In this study, 33 host proteins interacting with nsp1α were identified using yeast two-hybrid (Y2H), The interactions were further confirmed by co-immunoprecipitation (Co-IP) and confocal microscopy. Overexpression of PSMB4 reduced PRRSV nsp1α and N protein levels, while PRRSV infection did not affect PSMB4 expression. S146 and M148 within the mature chain domain of PSMB4 were found crucial for binding and reducing nsp1α levels. Future research will focus on exploring interactions of viral nsp1α with other host factors and their biological significance.

Materials and methods

Plasmids and cell lines

The bait plasmid for the yeast library screen was constructed using a traditional method. The complementary DNA (cDNA) sequence from the classical CH-1a strain of PRRSV was used to amplify the full-length nsp1α by PCR with specific primers listed in Supplemental Table S1. The resulting amplicons were then cloned into the yeast pGBKT7 vector using *EcoRI* and *BamHI* restriction sites to express the Gal4 DNA-binding domain fusion proteins.

The cDNA libraries for porcine lung tissue were separately constructed using gateway technology and cloned into the pGADT7-Rec vector through gene recombination techniques.

The cDNA sequence encoding the full-length gene was obtained through reverse transcription PCR (RT-PCR) and subsequently cloned into the pGADT7 yeast vector, with specific *EcoRI* and *XhoI* restriction sites added to the primer termini.

Marc-145 and HEK293T cells were previously stored in the laboratory and cultured in Dulbecco's Modified Eagle Medium (DMEM; Gibco, NY, USA) supplemented with 10% fetal bovine serum (FBS). PAMs were isolated from lung tissues and cultured in RPMI 1640 (Gibco) medium supplemented with 10% FBS. All cells were maintained at 37 °C in a 5% CO_2 incubator. All experiments were conducted in the Level 2 Biosafety Laboratory of the College of Veterinary Medicine, South China Agricultural University.

Yeast two-hybrid (Y2H) screening assays

In the Y2H assays, a porcine lung tissue cDNA library was screened for host proteins interacting with nsp1α using the GAL4 system, following the protocol outlined in the BD Matchmaker Library Construction and Screening Kits User Manual (Clontech, Palo Alto, CA). PRRSV nsp1α was inserted into the pGBKT7 yeast vector as bait and co-transformed with the lung tissue cDNA library into Y2H Gold cells. Transformants were cultured on SD/-Leu/-Trp/-His (TDO) medium and then selected for positive clones on SD/-Ade/-Leu/-Trp/-His (QDO/X/A) medium supplemented with X-α-gal and aureobasidin A (AbA). To validate protein interactions, full-length CDS sequence from pigs was cloned into the pGADT7 vector and co-transformed with pGBKT7-nsp1α into Y2H Gold cells. Transformants were grown on SD/-Leu/-Trp (DDO) for three days, then transferred to QDO/X/A medium with 70 μg/ml X-α-gal and 0.5 μg/ml AbA. pGBKT7-53 and pGADT7-T served as positive controls, while pGBKT7-Lam and pGADT7-T

were used as negative controls. Results were confirmed in three independent experiments.

Detection of self-activation and toxicity

pGBKT7-nsp1α and the blank vector pGADT7-T were co-transformed into Y2H cells. The transformants were separately grown on DDO/X, TDO/X and QDO/X/AbA screening media.

Western blot analysis

Cell samples cultured on 6/12-well plates were lysed using RIPA buffer (high) (Solarbio) according to the manufacturer's instructions. The cell lysates were then subjected to ultrasonic disruption and centrifuged at 12,000 rpm for 10 min. The supernatants were transferred to 500 μL sterile tubes, mixed with 5 × SDS-PAGE loading buffer, boiled for 10 min, and placed on ice for 2 min. Proteins of different molecular weights were separated using SDS-polyacrylamide gel electrophoresis (SDS-PAGE) with a One-Step PAGE Gel Fast Preparation Kit (Vazyme Biotechnology). The separated proteins were transferred onto a PVDF membrane using the semi-dry transfer method. After the membrane was blocked with 5% nonfat dry milk containing 0.1% Tween 20 for 1 h at room temperature, it was incubated overnight at 4 °C with a specific primary antibody or endogenous antibody. This was followed by incubation with the corresponding secondary antibody, HRP-labeled anti-mouse/rabbit IgG, for 1 h at room temperature. Finally, the membranes were visualized using the Amersham ImageQuant 800 (Cytiva, Washington, DC, USA).

Co-IP assays

In the Co-IP experiment, cell samples cultured on 6-well plates were lysed on ice for 30 min using 250 μL of cell lysis buffer (Beyotime) containing 1 mM PMSF protease inhibitor. The samples were then subjected to ultrasonic disruption and centrifuged at 12,000 rpm for 15 min. A small portion of the supernatant was used for input detection, while the majority was incubated with protein A/G magnetic beads (Selleck) to bind the specific antibody, according to the manufacturer's instructions. The antigen and antibody complex were incubated for 2 h at room temperature, and the beads were washed more than five times with washing buffer (50 mM Tris, 150 mM NaCl, 0.5% detergent, pH 7.5). Finally, 40 μL of 1 × SDS-PAGE loading buffer was added to the beads, followed by denaturation for 5 min at 100 °C, and the proteins were separated by SDS-PAGE for detection.

Confocal Immunofluorescence microscopy

HEK293T cells were cultured on coverslips in 12-well plates (1 × 10^5 cells) for approximately 12 h. The plasmids were co-transfected into the cells using a PEI transfection reagent, following the manufacturer's instructions. At 24 h post-transfection (hpt), cells were washed three times with phosphate-buffered saline (PBS), then fixed with 4% paraformaldehyde for 15 min at room temperature. Following three additional washes with PBS, cells were permeabilized with 1% Triton X-100 for 5 min, washed three more times and blocked with 1% bovine serum albumin at 37 °C for 1 h. After washing the cells three times, they were incubated with specific primary antibodies overnight at 4 °C. The cells were then washed with PBS and incubated with fluorescently conjugated secondary antibodies at room temperature for 1 h. After three more washes, the cells were stained with DAPI (4′, 6-diamidino-2-phenylindole) to visualize the cell nuclei. Finally, the cells were washed with phosphate-buffered saline (PBS), and images were captured using a Leica TCS SP8 laser confocal microscope (Germany).

Extraction of total cellular RNA and quantitative real-time PCR (qPCR)

HEK293T or Marc-145 cells cultured on 6-well plates were lysed with 1 mL of RNA isolator Total RNA Extraction Reagent (Vazyme, Nanjing, China) according to the manufacturer's instructions. Total RNA was isolated from the upper aqueous phase and precipitated with isopropyl alcohol. The RNA concentration and quality were measured using an Ultramicro nucleic acid protein analyzer. One microgram of total RNA was used to synthesize cDNA and qPCR was performed using 2 × ChamQ Universal SYBR qPCR Master Mix reagent (Vazyme, Nanjing, China) following the product's instructions.

RNA interference (RNAi)

Small interfering RNAs (siRNAs) were designed based on coding sequence (CDS) regions and synthesized by SYNBIO Technologies, Suzhou, China (Supplemental Table S1). Three siRNAs targeting PSMB4 were designated as siPSMB4-1, siPSMB4-2 and siPSMB4-3. These siRNAs, along with a non-targeting control siRNA (siNC), were individually transfected into Marc-145 cells using Lipofectamine 2000 (Lip2000) transfection reagent. At 48 hpt, the cells were collected for western blot analysis.

Statistical analysis

All experiments were performed with at least three biological replicates. Valid qPCR data were analyzed using the Student's t-test to compare two groups. Statistical significance between groups was considered when the p-value was less than 0.05 for all tests.

Results

PRRSV nsp1α exhibits no self-activation in Y2H screening assays

To identify host proteins that interact with nsp1α, the classical Y2H method was utilized in the screening assays. Nsp1α is translated from a single open reading frame (ORF) as a polyprotein, which is then self-cleaved to produce distinct proteins. The full-length sequence of nsp1α was inserted into the library bait vector pGBKT7. Self-activation test results indicated that co-transforming pGBKT7-nsp1α with pGADT7-T yielded a few colonies on the TDO/X medium, but no yeast growth occurred on the QDO/X/A solid media (Fig. 1A). Under these conditions, the Y2H screening assays using pGBK-nsp1α as bait were performed on the most stringent QDO/X/A nutritional deficiency screening medium (Fig. 1B).

Thirty-three potential host proteins interacting with nsp1α are screened

To maximize the screening of host proteins interacting with nsp1α, co-transformed clones were cultured on QDO/X/A medium plates. In the nsp1α screening experiment, a total of 128 clones turned blue, of which 60 were randomly selected for successful sequencing (including 9 sequencing doublets). Table 1 presents 33 potential binding partners with nsp1α identified from the porcine lung tissue cDNA library. Information on proteins interacting with nsp1α is listed in Table 1.

GO enrichment and KEGG pathway enrichment analysis

To further investigate the role of nsp1α in host cells, particularly in how it evades host immune responses and facilitates viral replication through interactions with host proteins, we performed Gene Ontology (GO) functional enrichment and Kyoto Encyclopedia of Genes and Genomes (KEGG) pathway enrichment analyses on 33 host proteins identified from nsp1α bait screening.

The GO molecular function analysis revealed that the majority of proteins interacting with nsp1α are involved in cell adhesion molecular binding, catalytic activity, and kinase binding activity (Fig. 2A). The biological process analysis showed significant enrichment in processes such as extracellular matrix organization, regulation of cell-substrate adhesion, response to abiotic stimuli, hemopoiesis regulation, and development (Fig. 2B). The cellular component analysis highlighted the presence of these interacting proteins in collagen-containing extracellular matrices, postsynaptic sites, and membrane rafts (Fig. 2C). Additionally, KEGG pathway analysis indicated that these proteins are primarily associated with viral infectious diseases, transport and catabolism, the host immune system, and signal transduction (Fig. 2D). Furthermore, several proteins were found to regulate channel activity, receptor activity, and enzyme activity. In summary, the interaction of PRRSV nsp1α with various host proteins suggests that these viral proteins may facilitate immune evasion by modulating diverse cellular signals and pathways.

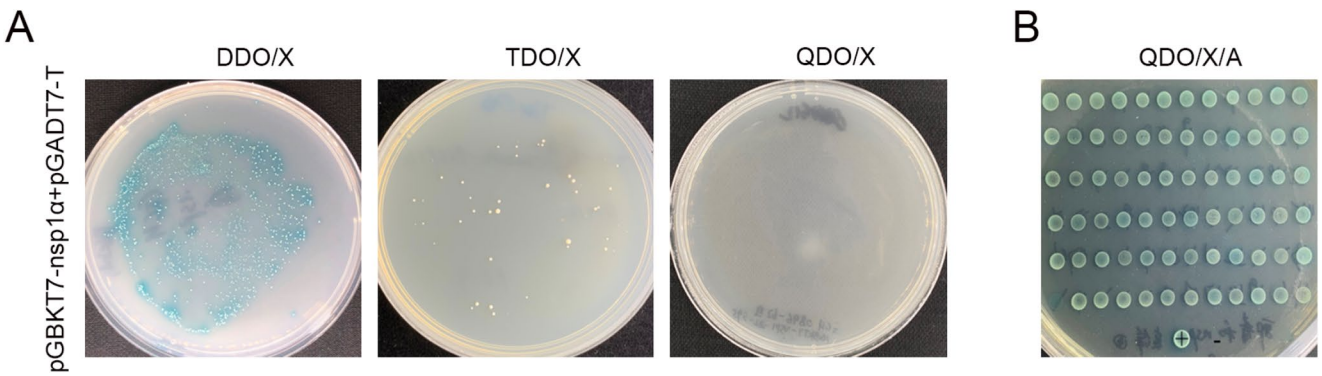

Fig. 1 Detection of self-activation of pGBKT7-nsp1α bait and screening host proteins interacting with nsp1α in Y2H assay. **(A)** pGBKT7-nsp1α bait plasmid was co-transformed with pGADT7-T into Y2H Gold cells and cultured on selective media. **(B)** Screening of nsp1α bait on QDO/X/A plates. DDO/X: media lacking Leu and Trp, but containing X-α-gal; TDO/X: media lacking Leu, Trp, and His, but containing X-α-gal; QDO/X: media lacking Ade, His, Leu and Trp, supplemented with X-α-gal; QDO/X/A: media lacking Ade, His, Leu and Trp, supplemented with X-α-gal and AbA

Table 1 Information on the 33 potential proteins interacting with PRRSV nsp1α

No	ID	Name	Gene symbol
1	XP_020922812.1	collagen alpha-1(I) chain isoform X1	COL1A1
2	XM_001929027.3	fibulin 5, transcript variant X3	FBLN5
3	XP_013843801.1	L-lactate dehydrogenase B chain isoform X1	LDHB
4	NP_001230636.1	cytosolic non-specific dipeptidase 2	CNDP2
5	XP_020925042.1	fibulin-2 isoform X2	FBLN2
6	NP_001231384.1	proteasome subunit beta type-4	PSMB4
7	XM_021080739.1	filamin A, transcript variant X16	FLNA
8	NM_001001771.1	fibrillin 1	FBN1
9	XM_001927002.7	WD repeat domain 61 transcript variant X1	WDR61
10	XM_021072336.1	bone morphogenetic protein 1	BMP1
11	XP_020939685.1	scaffold attachment factor B2 isoform X2	SAFB2
12	XP_020923614.1	microfibril-associated glycoprotein 4	MFAP4
13	EDL37305.1	elastin microfibril interfacer 1, isoform CRA	Emilin1
14	NP_001233144.1	ubiquitin/ISG15-conjugating enzyme E2 L6	UBE2L6
15	XP_003123103.1	amyloid beta A4 precursor protein-binding family A member 3	APBA3
16	BAM75557.1	IgG heavy chain precursor	IGHG
17	XP_020932614.1	slit homolog 3 protein isoform X3	SLIT3
18	XP_003127376.1	reticulocalbin-3	RCN3
19	CAN13328.1	major histocompatibility complex, class II, DR beta 1	HLA-DRB1
20	AAB69340.1	MHC class I antigen	PA1
21	XP_013838450.1	hermansky-pudlak syndrome 4 protein isoform X4	HPS4
22	NP_001230584.1	collagen alpha-2(I) chain precursor	COL1A2
23	AAA31124.1	SLA-DR-beta class II light chain	SLA-DRB1
24	XP_013849717.2	membrane-spanning 4-domains subfamily A member 4 A isoform X1	MS4A4A
25	XM_003125303.4	elastin microfibril interfacer 1	EMILIN1
26	XM_021090523.1	cysteine and histidine-rich protein 1	CYHR1
27	XM_003127015.4	CCAAT/enhancer binding protein alpha	CEBPA
28	XM_021096136.1	elastin microfibril interfacer 2	EMILIN2
29	XM_005666170.3	lysyl oxidase-like 1	LOXL1
30	XM_021094521.1	RELB proto-oncogene, NF-kB subunit	RELB
31	XP_003125105.1	poly(rC)-binding protein 1	PCBP1
32	XM_021080244.1	interferon regulatory factor 1	IRF1
33	AK395310.1	DnaJ heat shock protein family (Hsp40) member B1	DNAJB1

Co-localization of nsp1α with multiple host proteins

To further determine whether nsp1α interacts with the potentially identified proteins, we selected three functionally diverse proteins, including PSMB4, carnosine dipeptidase 2 (CNDP2) and poly(rC) binding protein 1 (PCBP1). Their coding sequences from *Chlorocebus sabaeus* were cloned into the expression vector pcDNA3.1, fused with a Myc tag at the C-terminus. HEK293T cells were separately co-transfected with nsp1α-mCherry and each of the four host proteins. After 24 h post-transfection, an indirect immunofluorescence assay (IFA) was performed using a Myc antibody, and the cell nuclei were stained with DAPI. Confocal fluorescence microscopy revealed that nsp1α-mCherry and mCNDP2-Myc exhibited overlapping yellow fluorescence in the cytoplasm. Conversely, nsp1α-mCherry and mPCBP1-Myc displayed overlapping yellow fluorescence in the cell nucleus (Fig. 3A).

Validation of the interaction between nsp1α and PSMB4

Among the screened proteins, PSMB4 stands out as an important factor involved in regulating the structure and function of the 26 S proteasome. To better understand the interaction between nsp1α and host proteins, we then focused on PSMB4. The PSMB4 sequence from pigs was cloned into the pGBKT7 vector, and its interaction with nsp1α was tested in yeast assays (Fig. 4A). Additionally, HEK293T cells were co-transfected with pPSMB4-Myc or mPSMB4-Myc and nsp1α-mCherry plasmids for 24 h, and anti-Myc or anti-mCherry immunoprecipitation assays were performed. Western blot analysis detected both nsp1α and PSMB4 in the precipitates (Fig. 4B, C, E & F). Notably, the endogenous interaction between nsp1α and monkey PSMB4 was confirmed by Co-IP in PRRSV-infected Marc-145 cells (Fig. 4H). Consistently, pPSMB4-Myc or

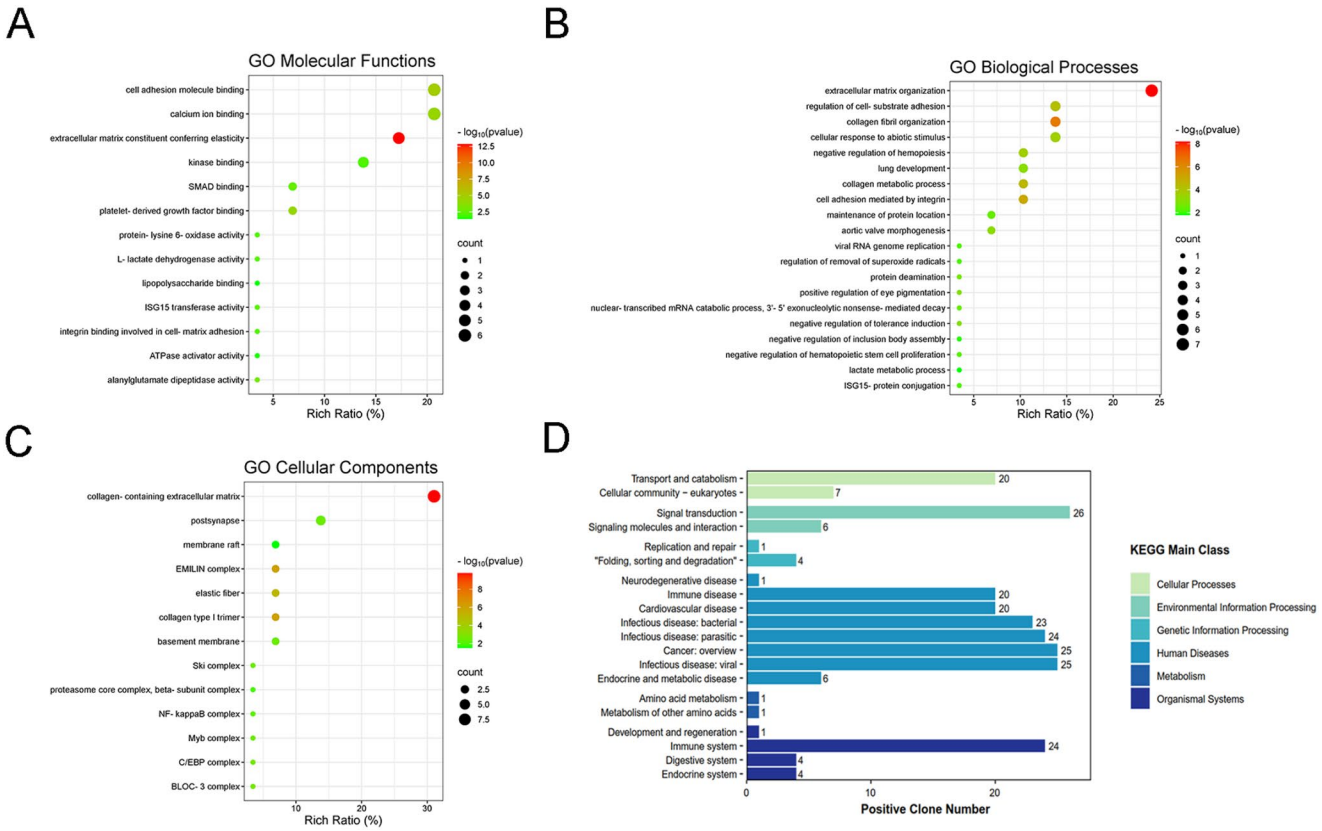

Fig. 2 The analysis of GO and KEGG enrichment. **(A)** GO molecular function analysis of interacting proteins from nsp1α bait screening. **(B)** GO biological process analysis of interacting proteins from nsp1α bait screening. **(C)** GO cellular component analysis of interacting proteins from nsp1α bait screening. **(D)** KEGG pathway analysis of interacting proteins from nsp1α bait screening

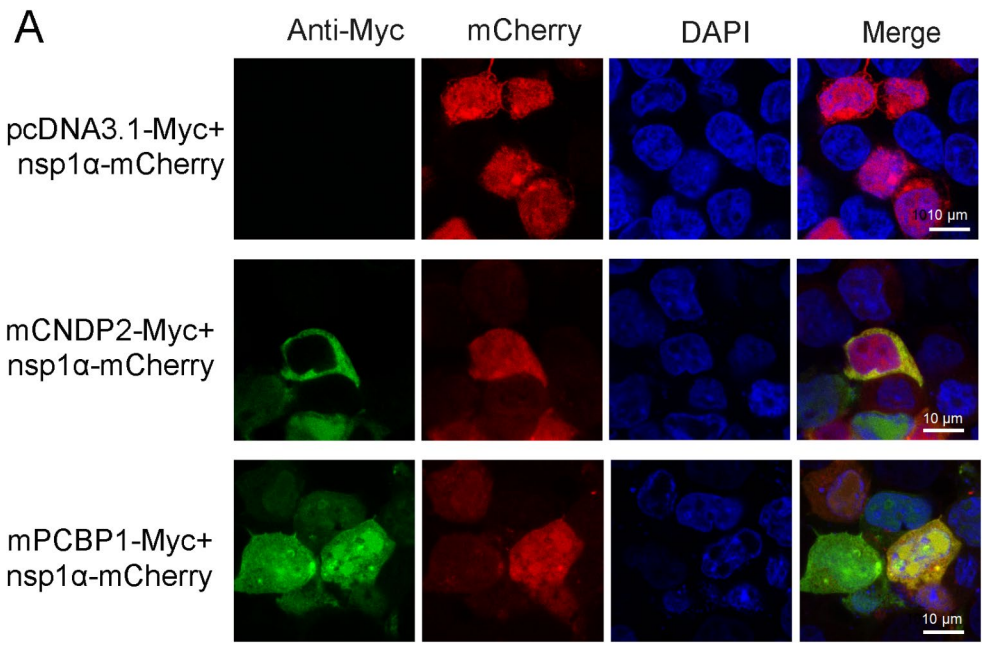

Fig. 3 Confocal fluorescence microscopy confirmed that nsp1α colocalizes with host proteins CNDP2 and PCBP1. **(A)** HEK293T cells were co-transfected with mCNDP2-Myc or mPCBP1-Myc and nsp1α-mCherry plasmids, with Myc empty vector and nsp1α-mCherry serving as controls. At 24 hpt, cells underwent indirect immunofluorescence analysis and were visualized using confocal microscopy. Scale bars, indicated by white lines, are shown. "m" represents the species of monkey

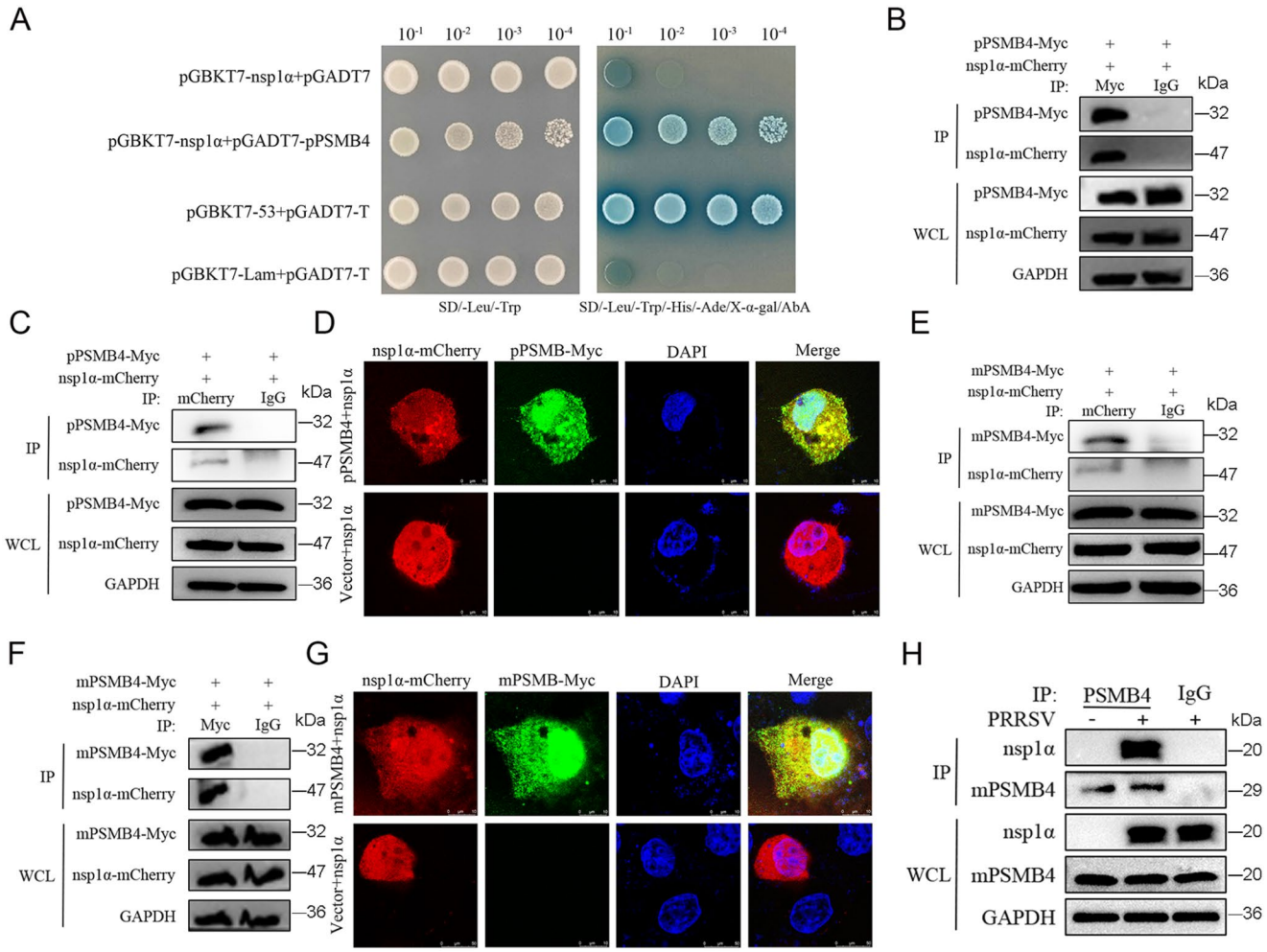

Fig. 4 Interactions between nsp1α and pPSMB4 or mPSMB4 were evaluated using Co-IP and co-localization assays both in vivo and in vitro. **(A)** Yeast transformants of nsp1α and pPSMB4 were grown on DDO and QDO nutritional deficiency media containing X-α-gal and AbA as screening supplements, whereas the control and negative groups did not grow. **(B, C, E & F)** Co-transfection of pPSMB4-Myc or mPSMB4-Myc with nsp1α-mCherry into HEK293T cells for 24 h. Cells were lysed using IP buffer, and total proteins were incubated with anti-Myc or anti-mCherry antibodies conjugated to magnetic beads. IP results were analyzed via western blot. "p" represents the species of pig, "m" represents monkey. **(D & G)** HEK293T cells were transfected with pPSMB4-Myc or mPSMB4-Myc and nsp1α-mCherry, with co-transfection of PSMB4-Myc and an empty vector serving as controls. At 24 hpt, cells underwent indirect immunofluorescence to detect PSMB4 (green) with anti-Myc antibody and nsp1α-mCherry (red) with anti-mCherry antibody. Cell nuclei were counterstained with DAPI (blue). Merged yellow fluorescence indicates the presence of colocalization, whereas scatterplot points visible to the eye indicate the absence of colocalization. **(H)** Marc-145 cells were infected with PRRSV, with uninfected (Mock) cells used as a control. At 36 hpi, total proteins were extracted using IP lysis buffer, and anti-mPSMB4 antibody was used for immunoprecipitation; nsp1α antibody was used to detect nsp1α protein bound to mPSMB4 protein

mPSMB4-Myc co-localized with nsp1α-mCherry in the cell nucleus (Fig. 4D & G). Taken together, these results strongly support the validity of screening nsp1α-interacted proteins from the natural host pig cDNA library.

PRRSV infection does not affect PSMB4 transcription and translation

To assess whether PSMB4 expression is influenced by PRRSV, we evaluated the accumulation of PSMB4 mRNA and protein levels during PRRSV infection. Marc-145 cells, cultured on 12-well plates to 100% confluency, were infected with PRRSV at a multiplicity of infection (MOI) of 0.5 for 0, 6, 12, 24 to 36 h. Uninfected cells served as controls. Both total RNA and protein were analyzed using qPCR and western blot. The results indicated that the accumulation of PSMB4 mRNA and protein was consistent across PRRSV-infected time points from 0 to 36 h and in uninfected groups (Fig. 5A, B & C). Additionally, varying PRRSV titers (0, 0.05, 0.5, and 5.0 MOI) were used to infect Marc-145 cells. At 24 h post-infection (hpi), there were no differences in endogenous PSMB4 mRNA and protein levels despite the

gradual accumulation of N protein (Fig. 5D & E). Meanwhile, porcine alveolar macrophages were infected with PRRSV for 0, 6, 12, 24 and 36 h. Western blot analysis of PSMB4 protein levels showed no significant difference at these time points (Fig. 5F). Furthermore, increasing doses of nsp1α did not affect PSMB4 protein levels either by increase or decrease (Fig. 5G). These data demonstrate that PRRSV infection does not influence PSMB4 expression.

PSMB4 negatively regulates PRRSV replication by reducing nsp1α protein levels

We next investigated the role of PSMB4 in PRRSV infection. Two μg of mPSMB4-Myc or an empty vector plasmid was transfected into Marc-145 cells. At 12 hpt, the cells were infected with PRRSV for 36 h. Western blot analysis revealed that the accumulation of N and nsp1α proteins was significantly lower in the mPSMB4-Myc group compared to the empty vector control groups (Fig. 6A & C). Correspondingly, immunofluorescence assays demonstrated that overexpressing mPSMB4 substantially reduced the fluorescence

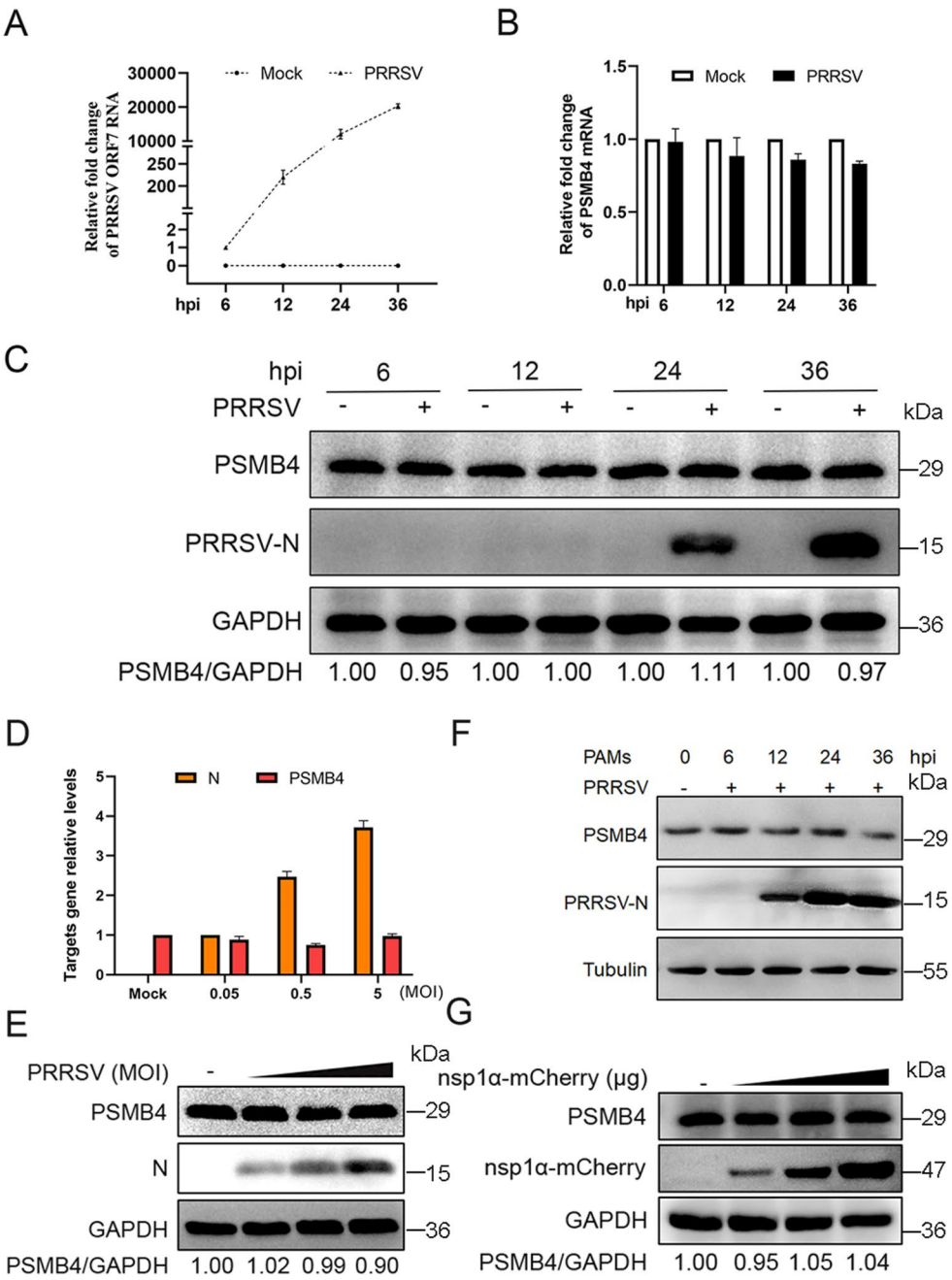

Fig. 5 PRRSV infection does not affect PSMB4 mRNA and protein expression. **(A-C)** Marc-145 cells (100% confluency) were infected with PRRSV (MOI = 0.5) for 6, 12, 24 and 36 h. Total RNA was extracted to analyze N and PSMB4 mRNA levels, and total protein was lysed to detect endogenous PSMB4, GAPDH, and N protein by western blot. **(D & E)** Endogenous PSMB4 protein expression at different MOI levels of PRRSV infection was analyzed by western blot, and N gene and PSMB4 mRNA expression were quantified by qPCR. **(F)** PAMs were infected with PRRSV for 6, 12, 24 and 36 h. Western blot analysis revealed the accumulation of PSMB4 protein. **(G)** Marc-145 cells were transfected with varying doses of nsp1α-mCherry plasmid for 24 h and western blot was used to analyze endogenous PSMB4 protein expression

accumulation of PRRSV N protein (Fig. 6B). Conversely, three siRNAs targeting PSMB4 and the negative control siRNA (siNC) were separately transfected into Marc-145 cells to knock down the endogenous PSMB4 gene. At 36 hpi, western blot analysis revealed that PSMB4 protein levels were lower compared to the control group, while PRRSV N protein accumulations were elevated (Fig. 6D). Collectively, these results suggest that PSMB4 acts as a negative regulator, inhibiting PRRSV replication during infection.

To further explore the biological significance of the interaction between PSMB4 and nsp1α, degradation assays were conducted by co-transfecting mPSMB4-Myc and nsp1α-mCherry plasmids in a dose-dependent manner into HEK293T cells, with co-transfection of an empty vector Myc and nsp1α-mCherry plasmid serving as the control. At 24 hpt, western blot analysis showed that the protein levels of nsp1α in the group co-expressing mPSMB4-Myc and nsp1α-mCherry were lower than in the control groups and decreased in a dose-dependent manner (Fig. 6E). This indicates that PSMB4 reduces nsp1α protein accumulation, thereby inhibiting PRRSV replication.

The mature chain of PSMB4 is crucial for binding and degrading nsp1α

To investigate the mechanisms by which PSMB4 degrades nsp1α dependent on their interaction, we explored which domain(s) of PSMB4 interact with nsp1α. PSMB4 consists of three functional structural domains: an N-terminal propeptide structure domain, a mature chain from positions 46 to 250 amino acids, and a C-terminal domain containing 14 amino acids (Fig. 7A). Three truncated mutants of PSMB4-ΔC-PSMB4 (lacking the C-terminal domain), ΔNΔC-PSMB4 (lacking both the propeptide and C-terminal domains) and ΔN-PSMB4 (lacking the N-terminal propeptide domain), in which all include the mature chain domain, were separately cloned into the pcDNA3.1 vector with a Myc-tag at the C-terminus. After co-transfecting these plasmids with nsp1α-mCherry into HEK293T cells for 24 h, a

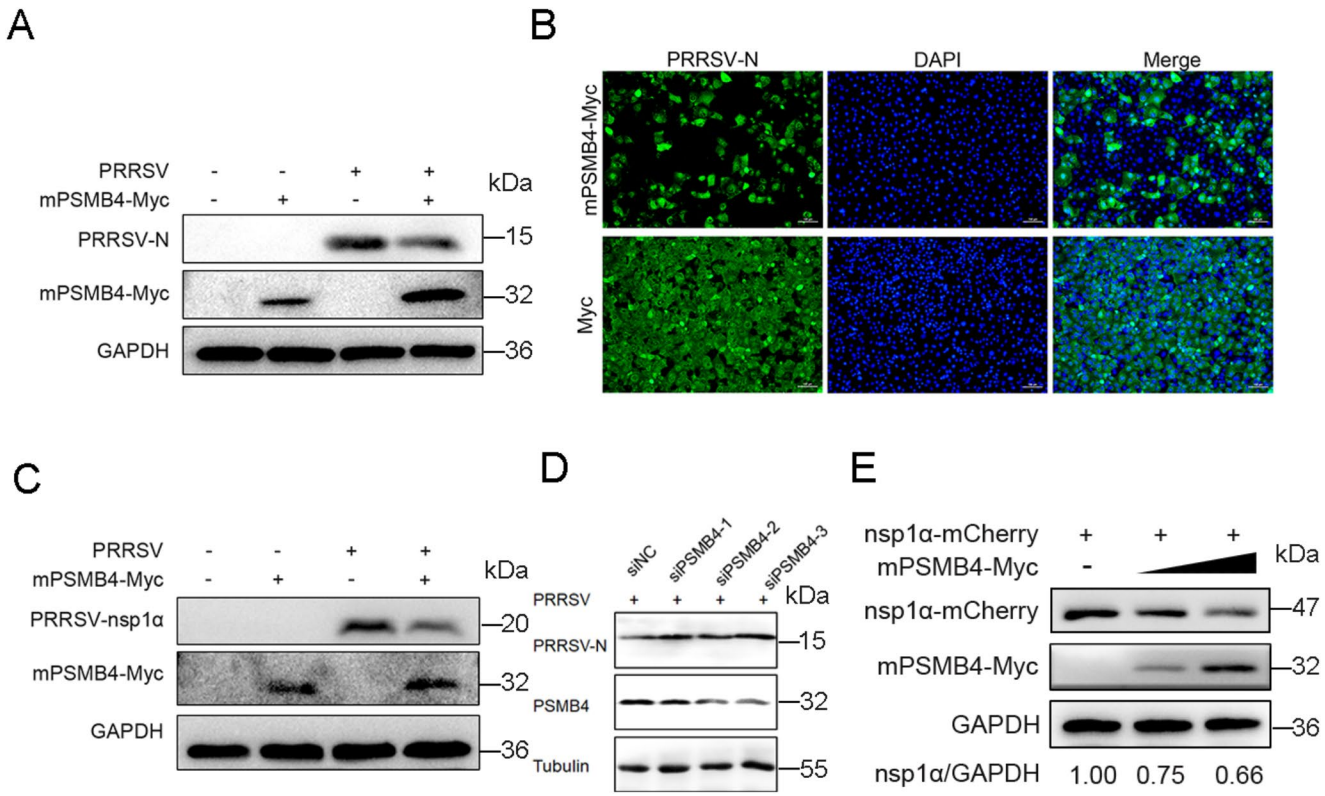

Fig. 6 PSMB4 negatively regulates PRRSV replication by down-regulating the expression of nsp1α protein. **(A)** 2 μg of PSMB4-Myc plasmid was transfected into Marc-145 cells; at 24 hpt, the cells were infected with PRRSV at an MOI of 0.5. At 36 hpi, N protein accumulation was analyzed, meanwhile at 24 hpi, N protein accumulation was assessed using indirect immunofluorescence. **(B)** N protein was detected with an anti-N antibody (green) and the nuclei were stained blue. Fluorescence images were captured at 10x magnification. **(C)** PSMB4-Myc was transfected into Marc-145 cells for 24 h, followed by PRRSV infection to assess nsp1α protein levels. **(D)** siRNAs targeting PSMB4 and the negative control siRNA (siNC) were transfected into Marc-145 cells. At 12 hpt, cells were inoculated with PRRSV and incubated for 36 h. Western blot analysis was performed to examine the accumulation of PRRSV N and PSMB4 proteins. **(E)** Co-transfection of PSMB4-Myc at varying doses with nsp1α-mCherry into HEK293T cells for 24 h was conducted to analyze exogenous nsp1α protein accumulation

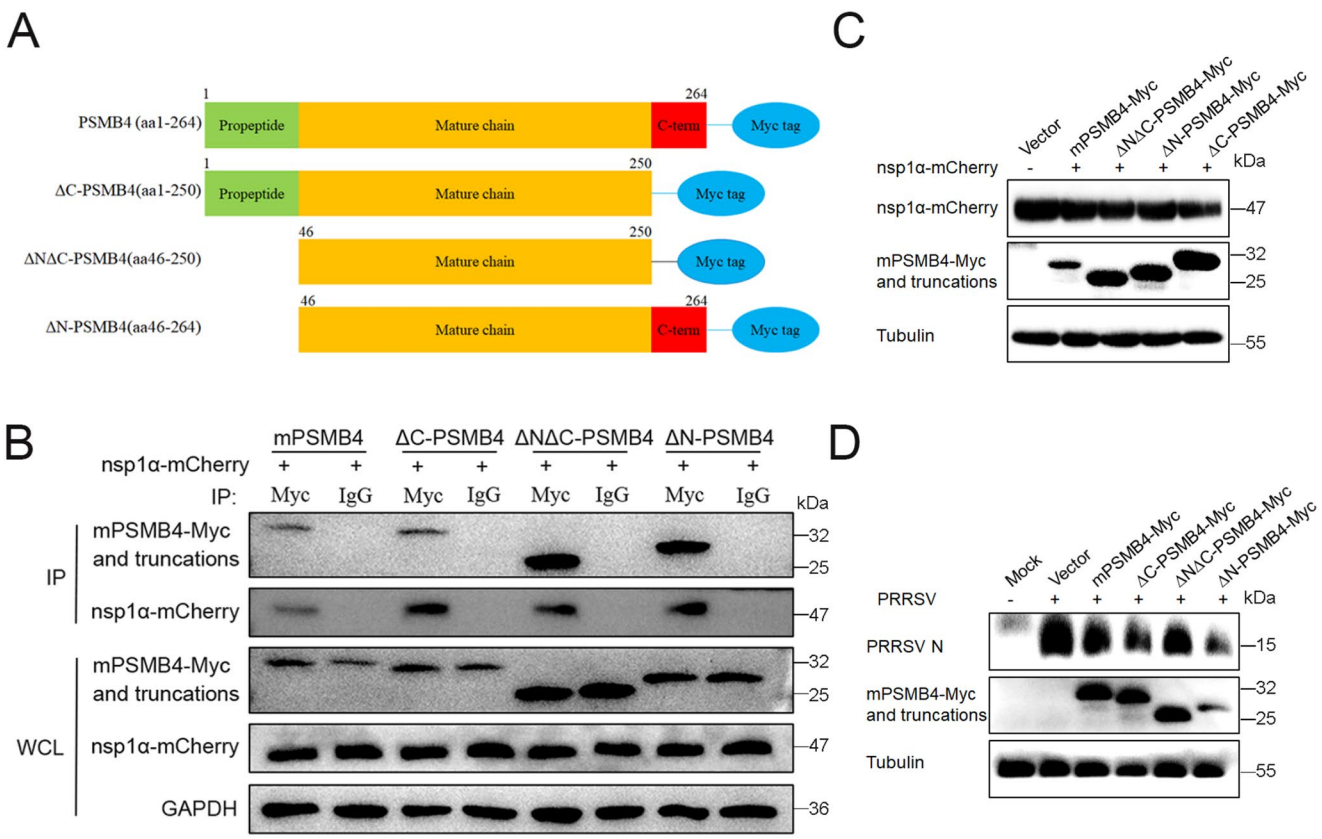

Fig. 7 PSMB4 degrades nsp1α through its mature chain domain. **(A)** A sketch map illustrates the conserved domains of PSMB4 (Green represents the propeptide domain, yellow the mature chain domain and red the C-terminal domain) and the construction of truncated mutant plasmids. **(B)** HEK293T cells in six-well plates were co-transfected with 2 μg of nsp1α and either ΔC-PSMB4, ΔNΔC-PSMB4, or ΔN-PSMB4. At 24 hpt, cell lysates underwent co-immunoprecipitation (Co-IP) using coupled Myc or IgG control antibodies, followed by immunoblotting with Myc and mCherry antibodies. **(C)** HEK293T cells were co-transfected with 2 μg of nsp1α and either ΔC-PSMB4, ΔNΔC-PSMB4, ΔN-PSMB4 or an empty plasmid. At 24 hpt, cell lysates were analyzed by western blot using corresponding Myc, mCherry or GAPDH antibodies. **(D)** Marc-145 cells were transfected with a single plasmid of PSMB4, ΔC-PSMB4, ΔNΔC-PSMB4, ΔN-PSMB4 or control Myc. At 12 hpt, cells were inoculated with PRRSV (MOI = 0.5) for an additional 36 h, after which cell lysates were analyzed by western blot using corresponding N, Myc or tubulin antibodies

Co-IP assay was conducted using anti-Myc and IgG control antibodies. Western blot analysis of the coprecipitates detected nsp1α and the three PSMB4 truncated mutants, indicating that nsp1α interacts with the mature chain domain of PSMB4 (Fig. 7B).

Next, we assessed whether the truncated mutants of PSMB4 could degrade nsp1α to inhibit PRRSV replication. HEK293T cells were co-transfected with the PSMB4 mutants using PEI transfection reagent in a degradation experiment. Western blot analysis revealed that nsp1α protein accumulation in cells expressing PSMB4 truncated mutants was lower than in control cells (Fig. 7C). Additionally, the PSMB4 truncated mutants and an empty vector control were individually transfected into Marc-145 cells using Lipofectamine 2000. Twelve h later, PRRSV (MOI = 0.5) was added to the treated cells. Western blot results showed that N protein accumulation in the truncated mutant groups was significantly lower than in the control group (Fig. 7D). Collectively, these findings confirm that the mature chain domain of PSMB4 is crucial for degrading nsp1α, thus limiting virus replication.

Amino acid residues S146 and M148 within PSMB4 mature chain domain are crucial for binding and degrading nsp1α

To elucidate the interaction between nsp1α and PSMB4 from a structural perspective, the AlphaFold3 server was utilized to predict the structures of nsp1α and PSMB4 (Fig. 8A & B). Additionally, Gramm-x online software (http://gramm.compbio.ku.edu/) was used to construct Z-docking models for these two proteins. Furthermore, PDBePISA online analysis was employed to examine interfaces and assemblies, aiming to identify key amino acid residues involved in binding (Fig. 8C & D). Through analysis of the protein structures and docking models, two amino acids in the

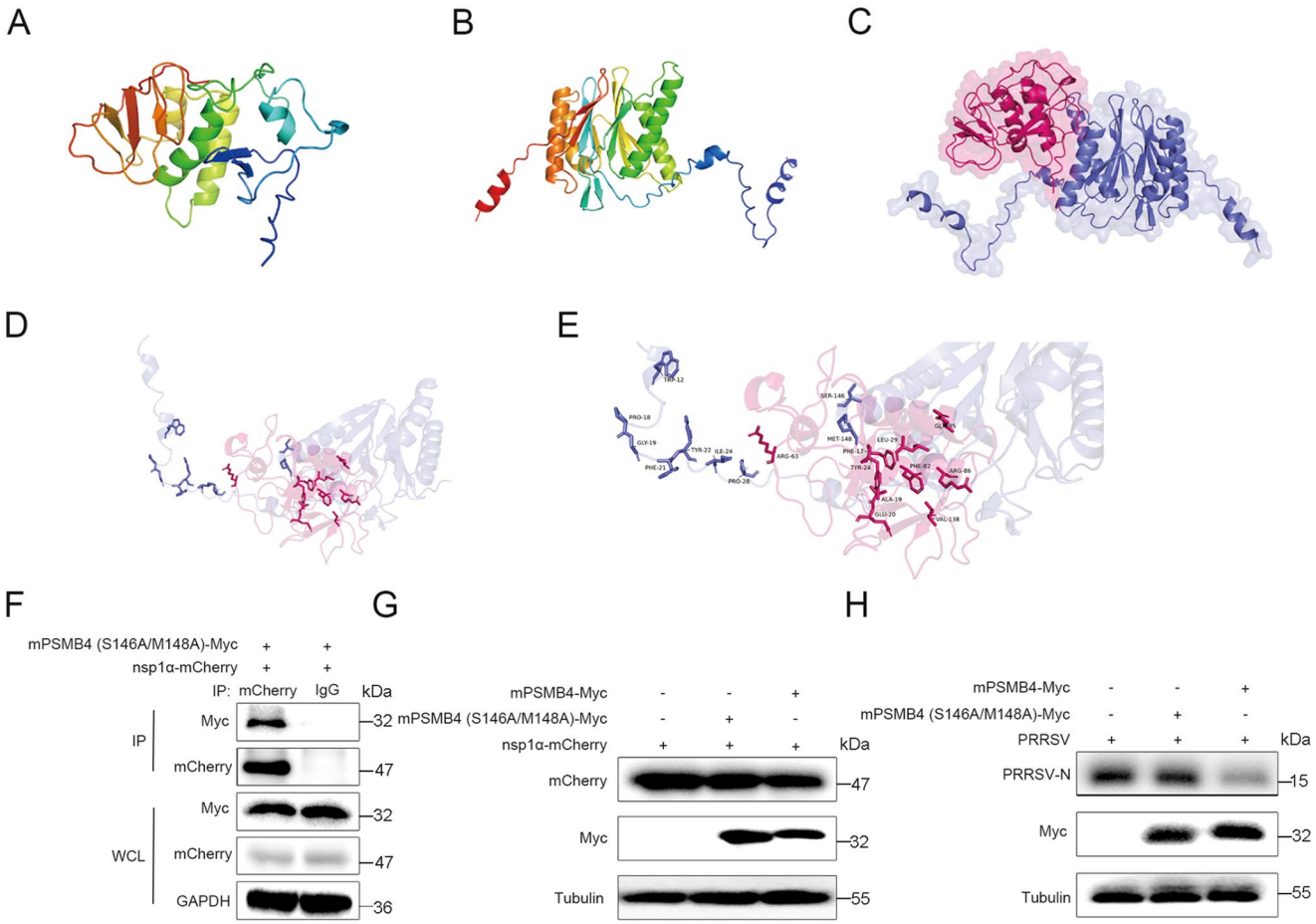

Fig. 8 Predicting key amino acid residues for PSMB4 binding to nsp1α. **(A)** The overall spatial structure of nsp1α. **(B)** The overall spatial structure of *Chlorocebus sabaeus* PSMB4. **(C)** The overall spatial structure of the nsp1α-PSMB4 complex, with the nsp1α backbone rendered in cartoon style and colored dark red, and PSMB4 in blue. **(D & E)** Z-docking results illustrate the interaction between the PSMB4 (blue) and nsp1α protein (dark red). **(F)** Co-transfecting the double site mutants of mPSMB4 and nsp1α-mCherry into the HEK293T cells for 24 h, anti-Myc and control anti-IgG were used as IP and western blot detected the relative proteins. **(G)** HEK293T cells were co-transfected with nsp1α-mCherry and empty vector, double site mutants of mPSMB4 or wild-type mPSMB4, western blot analyzed protein accumulations. **(H)** co-transfecting nsp1α-mCherry and empty vector, double site mutants of mPSMB4 or wild-type mPSMB4 into Marc-145 cells, at 12 hpt, the cells were inoculated PRRSV for 36 h and lysed to analysis the protein accumulations

PSMB4 spatial structure, S146 and M148, were identified as potential mediators of interactions with critical residues in nsp1α, as indicated by a negative change in Gibbs free energy (ΔiG < 0) (Fig. 8E).

To confirm the reliability of structure prediction and further explore the specific amino acid site of nsp1α degraded by PSMB4. Based on the above structural prediction results, we simultaneously mutated S146 and M148 to alanine within the mature chain domain of PSMB4, to obtain PSMB4 (S146A/M148A)-Myc recombinant plasmid. When PSMB4 (S146A/M148A)-Myc and nsp1α-mCherry were co-transfected into HEK293T cells, Co-IP results showed that only the IP: Myc group could detect specific nsp1α bands (Fig. 8F), suggesting that S146 and M148 within PSMB4 may not be the only sites binding to nsp1α. To determine whether S146 and M148 mutations cause functional changes, HEK293T cells were co-transfected with nsp1α-mCherry and Myc, PSMB4 (S146A/M148A)-Myc and PSMB4-Myc, respectively. The results showed that the accumulation of nsp1α protein in the PSMB4 mutant group was lower than that in the no-load control group, but significantly higher than that in the PSMB4 wild-type group (Fig. 8G). The results showed that the simultaneous mutation of S146 and M148 alleviated the degradation of nsp1α mediated by PSMB4. Interestingly, mutations at S146 and M148 within the mature chain domain of PSMB4 partially relieved its inhibition on PRSSV replication (Fig. 8H). These results indicate that amino acid residues S146 and M148 within the mature chain of PSMB4 play an important role in the introduction of binding and degradation of nsp1α.

Discussion

PRRS is widely popular in the global pig industry due to its high genetic variability and widespread prevalence, leading to huge economic losses. The pathogen PRRSV has demonstrated a capacity for mutation and recombination, which leads to the emergence of new, more virulent strains [7]. In this case, current vaccines offer only partial protection and may fail to prevent the spread of emerging variants like NADC30. From host genetic view, screening interacted proteins involved in host resistance or susceptibility is an effective strategy. To achieve this, a deeper understanding of virus-host interactions involved in immunomodulation is required.

In this study, thirty-three putative host factors interacting with PRRSV nsp1α were screened by classical and valid Y2H method. The Y2H system is one of the most virtual interacted partners screening ways because it can screen interactions within many proteins simultaneously and interactions may be more representative of physiological conditions compared to in vitro assays. The interacting host proteins are involved in either host immune, transport and catabolism, signal transduction and infectious disease caused by viruses, or have been reported to be targeted by PRRSV and other viruses. For example, Hermansky-Pudlak syndrome 4 protein isoform X4 (HPS4) is primarily associated with lysosome-related organelles, and plays a role in protein trafficking and organelle biogenesis, specifically through its involvement in the biogenesis of lysosome-related organelles complex (BLOC)-3 [26]. Reticulocalbin-3 (RCN3) is a protein primarily involved in calcium-binding within the endoplasmic reticulum (ER). It helps regulate protein folding and secretion, processes that are critical during viral infections [27, 28]. Ubiquitin/ISG15-conjugating enzyme E2 L6 (UBE2L6), also known as UBCH8, plays a role in the ISGylation process, which is an important part of the host antiviral response [29, 30]. The WD repeat domain 61 (WDR61) protein is part of a broader family of WD-repeat proteins known for their role in protein-protein interactions, often functioning in complex cellular processes, such as transcriptional regulation [31, 32]. IRF1 is a transcription factor critical for inducing type I interferon (IFN) responses, particularly in response to viral infections. It helps regulate the expression of IFN-β and IFN-stimulated genes, which are key to antiviral defenses [33]. These are often targeted by viruses to evade immune detection, so next study would focus on these proteins when searching for known literature.

PSMB4 was identified in previously reported interactions, which is involved in degrading unneeded or damaged proteins by proteolysis. Yi et al. reported that PSMB4 plays a role in the degradation of nsp1α through the autolysosome pathway. The mechanistic study found PSMB4 was involved in the early steps of marking protein nsp1α for degradation, which not only reduced viral replication by removing essential viral proteins but also had downstream effects on immune signaling pathways, notably the type I interferon (IFN) pathway [25]. In this study, we also confirmed that nsp1α interacts with pig and monkey PSMB4 using Y2H, Co-IP and confocal microscopy. Our study found that three truncated mutants of PSMB4 containing the mature chain domain all interact with the full-length nsp1α. Immunoprecipitation results showed that when using PSMB4 mutants to precipitate nsp1α, nsp1α was also detected in the precipitate of the mutant containing the N-terminal polypeptide domain, which is inconsistent with the results reported by Yi et al. On one hand, we believe this discrepancy could be due to the use of different PRRSV strains. In our study, all experiments were performed with the classic PRRSV strain CH-1a (accession number: EU807840.1), whereas Yi et al. used the highly pathogenic PRRSV strain XHGD (gene accession number: EU624117). Our findings demonstrate that the PSMB4 mature chain domain spanning residues 46–250 aa can interact with nsp1α to reduce nsp1α protein levels, thus inhibiting PRRSV replication. Spatial structure predictions suggest that PSMB4 interacts with nsp1α through amino acid residues S146 and M148 within its mature chain domain, and that many potential amino acid residues in nsp1α may interact with PSMB4. This indicates that the conserved mature chain domain of PSMB4 is a key component for binding and degrading nsp1α. On the other hand, this could also be a result of protein folding. In our experiment, nsp1α was expressed as a fusion with the mCherry tag protein, meaning nsp1α is expressed first, followed by the fusion tag. This could potentially affect the spatial structure of nsp1α, leading to its binding with PSMB4. The AlphaFold3 server is currently considered an effective tool for accurately predicting protein structures and protein-protein interactions. Our structural prediction results indicate that nsp1α interacts with PSMB4 at critical amino acid residues S146 and M148, which are located in the mature chain domain where PSMB4 interacts with nsp1α. This is consistent with our Co-IP results, which show that the mature chain domain of PSMB4 interacts with nsp1α. To confirm that S146 and M148 are the key interaction sites for PSMB4 binding to nsp1α, we constructed an expression plasmid in which S146 and M148 were simultaneously mutated and fused with a Myc tag at the C-terminus. Immunoprecipitation experiments showed that the PSMB4 mutant still interacts with nsp1α, suggesting that S146 and M148 within the mature chain domain may not be the only interaction sites between PSMB4 and nsp1α. However, degradation experiments revealed that the mutation of S146 and M148 significantly alleviates PSMB4-mediated degradation of nsp1α. Moreover, overexpression of the PSMB4 mutant leads to

a significant increase in PRRSV N protein accumulation, indicating that S146 and M148 within the mature chain domain play a crucial role in mediating PSMB4-induced degradation of nsp1α. This observation does not contradict the finding that the mutant still interacts with nsp1α. Thus, our results demonstrate that the predicted interaction sites S146 and M148 in PSMB4 play an important role in both binding and degrading nsp1α.

In the complex interaction between viruses and their hosts, host proteins can be hijacked by viral proteins to assist the virus in transcription, replication, and evasion of host immunity. In our yeast screening experiment, both L-lactate dehydrogenase B chain isoform X1 (LDHB) and PCBP1 were selected by nsp1α, suggesting that they may play an important role in the replication of PRRSV. Studies have shown that the multifunctional protein PCBP regulates various processes involved in the formation, assembly, and release of positive-strand RNA virus particles. Cousineau found that the RNA-binding protein PCBP binds to the 5' untranslated region of the Hepatitis C virus (HCV) and limits the assembly and secretion of HCV virions, with surface PCBP affecting the utilization of viral genomic RNA [34]. Nsp1α is the first protein synthesized by PRRSV and regulates sub-genomic RNA synthesis, and confocal microscopy has shown that PCBP strongly co-localizes with nsp1α in the cell nucleus, indicating that PCBP may hijack nsp1α to limit viral assembly. LDHB is an enzyme expressed in various tissues, primarily catalyzing the reversible conversion between lactate and pyruvate. Studies have shown that LDHB levels are significantly elevated in COVID-19 patients and are associated with the severity of the disease [35]. Elevated LDHB levels may reflect the metabolic response of the body to viral infections [36]. Therefore, PRRSV may promote infection by regulating LDHB metabolism through nsp1α, which is one of the directions of our future research.

Conclusions

The interaction between PRRSV nsp1α and host proteins was conducted using Y2H screening. We used nsp1α as bait, a total of 33 potential interacting proteins were identified. Among these candidates, we confirmed that nsp1α co-localized with host proteins PSMB4, CNDP2 and PCBP1. The interaction between nsp1α and PSMB4 was further validated through Y2H and Co-IP assays. PRRSV infection did not affect the mRNA and protein expression levels of PSMB4. However, overexpressing PSMB4 led to a decrease in the accumulation of viral nsp1α and N proteins. Furthermore, amino acids S146 and M148 within the mature chain domain of PSMB4 are critical for binding and degrading nsp1α.

Supplementary Information The online version contains supplementary material available at https://doi.org/10.1007/s00018-025-05679-9.

Author contributions Binghua Chen: Writing-original draft, Data curation, Conceptualization, Formal analysis. Binghua Chen and Yongjie Chen: Investigation, Methodology, Validation, Data curation. Zhan He: Structure analysis, Software, Validation, Data curation. Yanfei Pan, Yunyan Luo, Jiecong Yan and Fangfang Li: Validation, Data curation. Chunhe Guo: Conceptualization, Funding acquisition, Supervision, Writing-review & editing.

Funding This work was supported by the Basic and Applied Basic Research Foundation of Guangdong Province (2024A1515012991), the National Key Research and Development Program of China (2023YFD1801500), and the Science and Technology Planning Project of Guangzhou (2023B03J0947 and 2025D04J0072).

Data availability Data will be made available on request.

Declarations

Competing interest The authors declare no conflict of interest.

References

1. Kvisgaard LK, Hjulsager CK, Kristensen CS, Lauritsen KT, Larsen LE (2013) Genetic and antigenic characterization of complete genomes of type 1 Porcine reproductive and respiratory viruses (PRRSV) isolated in Denmark over a period of 10 years. Virus Res 178(2):197–205
2. Liu JK, Wei CH, Dai AL, Fan KW, Yang BH, Huang CF, Li XH, Yang XY, Luo ML (2017) Complete genomic characterization of two European-genotype Porcine reproductive and respiratory syndrome virus isolates in Fujian Province of China. Arch Virol 162(3):823–833
3. Wu ZY, Chang T, Wang DC, Zhang HL, Liu HZ, Huang XY, Tian ZJ, Tian XX, Liu D, An TQ, Yan Y (2024) Genomic surveillance and evolutionary dynamics of type 2 Porcine reproductive and respiratory syndrome virus in China spanning the African swine fever outbreak. Virus Evol 10(1):veae016

4. Laplana M, Estany J, Fraile LJ, Pena RN (2020) Resilience effects of SGK1 and TAP1 DNA markers during PRRSV outbreaks in reproductive sows. Anim (Basel) 10(5):902
5. Wang Y, Li R, Qiao SL, Wang JX, Liu HL, Li ZJ, Ma HF, Yang L, Ruan HY, Weng MY, Hiscox JA, Stewart JP, Nan YC, Zhang GP, Zhou EM (2020) Structural characterization of non-structural protein 9 complexed with specific nanobody pinpoints two important residues involved in Porcine reproductive and respiratory syndrome virus replication. Front Microbiol 11:581856
6. Thiel HJ, Meyers G, Stark R, Tautz N, Rumenapf T, Unger G, Conzelmann KK (1993) Molecular characterization of positive-strand RNA viruses: pestiviruses and the Porcine reproductive and respiratory syndrome virus (PRRSV). Arch Virol Suppl 7:41–52
7. Cui XY, Xia DS, Huang XY, Sun Y, Shi M, Zhang JQ, Li GW, Yang YB, Wang HW, Cai XH, An TQ (2022) Analysis of Recombinant characteristics based on 949 PRRSV-2 genomic sequences obtained from 1991 to 2021 shows that viral multiplication ability contributes to dominant recombination. Microbiol Spectr 10(5):e0293422
8. Liu BJ, Luo LZ, Shi ZQ, Ju HB, Yu LX, Li GX, Cui J (2023) Research progress of Porcine reproductive and respiratory syndrome virus NSP2 protein. Viruses 15(12):2310
9. Yoo DW, Song C, Sun Y, Du YJ, Kim O, Liu HC (2010) Modulation of host cell responses and evasion strategies for Porcine reproductive and respiratory syndrome virus. Virus Res 154(1–2):48–60
10. Li RQ, Chen C, He J, Zhang LL, Zhang L, Guo YY, Zhang WT, Tan K, Huang JH (2019) E3 ligase ASB8 promotes Porcine reproductive and respiratory syndrome virus proliferation by stabilizing the viral nsp1alpha protein and degrading host IKK beta kinase. Virology 532:55–68
11. Li W, Zhang MT, Wang YS, Zhao SJ, Xu PL, Cui ZY, Chen J, Xia PG, Zhang YN (2024) PRRSV GP5 inhibits the antivirus effects of chaperone-mediated autophagy by targeting LAMP2A. mBio 15(8):e0053224
12. Sun YN, Xue F, Guo Y, Ma M, Hao N, Zhang XC, Lou ZY, Li XM, Rao ZH (2009) Crystal structure of Porcine reproductive and respiratory syndrome virus leader protease nsp1α. J Virol 83(21):10931–10940
13. Xue F, Sun YN, Yan LM, Zhao C, Chen J, Bartlam M, Li XM, Lou ZY, Rao ZH (2010) The crystal structure of Porcine reproductive and respiratory syndrome virus nonstructural protein nsp1β reveals a novel metal-dependent nuclease. J Virol 84(13):6461–6471
14. Tijms MA, Nedialkova DD, Zevenhoven-Dobbe JC, Gorbalenya AE, Snijder EJ (2007) Arterivirus subgenomic mRNA synthesis and virion biogenesis depend on the multifunctional nsp1 autoprotease. J Virol 81(19):10496–10505
15. Song C, Krell P, Yoo DW (2010) Nonstructural protein 1alpha subunit-based Inhibition of NF-kappaB activation and suppression of interferon-beta production by Porcine reproductive and respiratory syndrome virus. Virology 407(2):268–280
16. Han MY, Du YJ, Song C, Yoo DW (2013) Degradation of CREB-binding protein and modulation of type I interferon induction by the zinc finger motif of the Porcine reproductive and respiratory syndrome virus nsp1alpha subunit. Virus Res 172(1–2):54–65
17. Beura LK, Sarkar SN, Kwon B, Subramaniam S, Jones C, Pattnaik AK, Osorio FA (2010) Porcine reproductive and respiratory syndrome virus nonstructural protein 1beta modulates host innate immune response by antagonizing IRF3 activation. J Virol 84(3):1574–1584
18. Zheng YH, Jiang DD, Sui C, Wu XJ, Hu Y, Lee CH, Cong XY, Li JT, Lu Y, Wang Z, Du YJ, Qi J, Huang J (2024) PRRSV nsp1alpha degrades TRIM25 through proteasome system to inhibit host antiviral immune response. Vet Microbiol 296:110173
19. Jing HY, Fang LR, Ding Z, Wang D, Hao WQ, Gao L, Ke WT, Chen HC, Xiao SB (2017) Porcine reproductive and respiratory syndrome virus nsp1alpha inhibits NF-kappaB activation by targeting the linear ubiquitin chain assembly complex. J Virol 91(3):e01911–e01916
20. Wang XD, Shao CY, Wang LY, Li QJ, Song HH, Fang WH (2016) The viral non-structural protein 1 alpha (Nsp1alpha) inhibits p53 apoptosis activity by increasing murine double minute 2 (mdm2) expression in Porcine reproductive and respiratory syndrome virus (PRRSV) early-infected cells. Vet Microbiol 184:73–79
21. Murata S, Yashiroda H, Tanaka K (2009) Molecular mechanisms of proteasome assembly. Nat Rev Mol Cell Biol 10(2):104–115
22. Tyedmers J, Mogk A, Bukau B (2010) Cellular strategies for controlling protein aggregation. Nat Rev Mol Cell Biol 11(11):777–788
23. Montenegro-Venegas C, Fienko S, Anni D, Pina-Fernandez E, Frischknecht R, Fejtova A (2020) Bassoon inhibits proteasome activity via interaction with PSMB4. Cell Mol Life Sci 78(4):1545–1563
24. Yang CH, Hsu CF, Lai XQ, Chan YR, Li HC, Lo SY (2022) Cellular PSMB4 protein suppresses influenza A virus replication through targeting ns1 protein. Viruses 14(10):2277
25. Yi HY, Wang QM, Lu LC, Ye RR, Xie EM, Yu ZQ, Sun YK, Chen Y, Cai MK, Qiu YW, Wu QW, Peng J, Wang H, Zhang GH (2023) PSMB4 degrades the Porcine reproductive and respiratory syndrome virus nsp1alpha protein via the autolysosome pathway and induces the production of type I interferon. J Virol 97(4):e0026423
26. Yokoyama T, Brien KJO, Franklin TM, Zuo BLG, Zuo MXG, Merideth MA, Introne WJ, Gochuico BR (2024) Impairment of renal function in hermansky-pudlak syndrome. Am J Nephrol 9:1–10
27. Shi XQ, An XJ, Yang L, Wu ZP, Zan DN, Li ZH, Pang BS, Chen Y, Li JJ, Tan PP, Ma RZ, Fang QH, Ma YM, Jin JW (2021) Reticulocalbin 3 deficiency in alveolar epithelium attenuated LPS-induced ALI via NF-kappaB signaling. Am J Physiol Lung Cell Mol Physiol 320(4):L627–L639
28. He Y, Alejo S, Johnson JD, Jayamohan S, Sareddy GR (2023) Reticulocalbin 3 is a novel mediator of glioblastoma progression. Cancers (Basel) 15(7):2008
29. Li L, Bai J, Fan H, Yan JF, Li SH, Jiang P (2020) E2 ubiquitin-conjugating enzyme UBE2L6 promotes senecavirus A proliferation by stabilizing the viral RNA polymerase. PLoS Pathog 16(10):e1008970
30. Orfali N, Shan-Krauer D, O'Donovan TR, Mongan NP, Gudas LJ, Cahill MR, Tschan MP, McKenna SL (2020) Inhibition of UBE2L6 attenuates isgylation and impedes ATRA-induced differentiation of leukemic cells. Mol Oncol 14(6):1297–1309
31. Hou YY, Zhang CY, Liu L, Yu Y, Shi L, Qin Y (2024) WDR61 ablation triggers R-loop accumulation and suppresses breast cancer progression. FEBS J 291(15):3417–3431
32. Barman P, Ferdoush J, Kaja A, Chakraborty P, Uprety B, Bhaumik R, Bhaumik R, Bhaumik SR (2024) Ubiquitin-proteasome system regulation of a key gene regulatory factor, Paf1C. Gene 894:148004
33. Wang JJ, Li HY, Xue BB, Deng RL, Huang X, Xu Y, Chen SW, Tian RY, Wang XT, Xun Z, Sang M, Zhu HZ (2020) IRF1 promotes the innate immune response to viral infection by enhancing the activation of IRF3. J Virol 94(22):e01231–e01220
34. Ngberg KS, Schwartz S (1999) Poly(C)-binding protein interacts with the hepatitis C virus 5' untranslated region. J Gen Virol 80(Pt 6):1371–1376
35. Monaco V, Iacobucci I, Cane L, Cipollone I, Ferrucci V, Antonellis Pde, Quaranta M, Pascarella S, Zollo M, Monti M (2024) SARS-CoV-2 uses Spike glycoprotein to control the host's

anaerobic metabolism by inhibiting LDHB. Int J Biol Macromol 278(Pt 3):134638
36. Fan SQ, Wu KK, Zhao MQ, Yuan J, Ma SM, Zhu E, Chen YM, Ding HX, Yi L, Chen JD (2020) LDHB Inhibition induces mitophagy and facilitates the progression of CSFV infection. Autophagy 17(9):2305–2324